Gaussian Circular 2D FIR Filters Designed Using Analytical Approach

RADU MATEI[1,2]
[1]Faculty of Electronics, Telecommunications and Information Technology
"Gheorghe Asachi" Technical University of Iaşi
Bd. Carol I no.11 A, Iaşi
[2]Institute of Computer Science, Romanian Academy – Iaşi Branch
ROMANIA

Abstract: - This paper proposes an analytical design procedure for a particular class of 2D filters, namely Gaussian-shaped FIR filters with circular symmetry. We approach both the low-pass and band-pass circular filters, which are adjustable in selectivity and peak frequency. The design starts from a specified 1D Gaussian prototype filter, approximated efficiently using Chebyshev series. A frequency transformation expressed in matrix form is applied to the prototype, generating the circular filter. These approximations and frequency mappings lead directly to the transfer function or frequency response of the circular filter with desired characteristics. Several relevant design examples are provided for both types of filters. The filters designed through this method are accurate in shape and efficient, of relatively low order, and their frequency response results in either a factored or nested form, convenient for implementation. Due to this parametric approach, the designed 2D filters are adjustable, therefore by changing the specifications, new 2D circular filters result in a straightforward manner and the design need not be resumed each time from the start, as generally is the case with most numerical optimization techniques.

Key-Words: - 2D FIR filters, approximations, Gaussian circular filters, analytic design

Received: February 1, 2020. Revised: August 7, 2020. Accepted: August 30, 2020. Published: September 16, 2020.

1 Introduction

Two-dimensional filters have constantly developed as an essential research field, due to their important applications in digital image processing, and various design techniques have been elaborated [1]. As an alternative to the well-known optimization methods based on numerical algorithms, generally leading to optimal filters for the imposed specifications, there have been also developed analytical design methods which have their advantages, such as a closed form of the filter frequency response and the tunability, or the capability to adjust filter characteristics through their parameters. These analytic design techniques rely on 1D prototypes, to which a specific frequency transformation is applied, depending on the desired 2D filter. A convenient and largely used tool for 2D filter design is also the McClellan transform [2], [3]. There exist a large variety of 2D filters with various shapes, both of FIR and IIR type which find specific applications in image processing. Circular filters are largely used due to their properties and many design methods have been developed in earlier and more recent papers such as [4]-[8]. Efficient design of anisotropic Gaussian filters is achieved in [9], [10]. Applications of the circular Gabor filters in texture segmentation are given in [11]. Some recent, novel filter design techniques are also found in [12], [13]. The author has approached analytical design of 2D FIR and IIR filters in previous works. Some circular filters were designed in [14], while in [15] and [16] circular filter banks, with applications in biomedical image filtering, are proposed. Directional and square IIR filters are described in [17]. Separable Gaussian directional FIR filters were approached in [18].

This work introduces an analytical design method of parametric circularly-symmetric 2D FIR filters, with a Gaussian shape. The novelty is that the resulted filters are adjustable through specified parameters, controlling the selectivity and the peak frequency for band-pass filters. The design process starts from a 1D prototype filter with factored transfer function, to which a specific frequency mapping is applied, leading directly to the desired 2D filter frequency response, which also results directly factored, thus allowing for convenient implementation. The paper is organized as follows: section 2 introduces the Gaussian prototype, approximated in section 3 as a trigonometric series, then as a polynomial; also a frequency mapping for circular filters is defined in matrix form. Several design examples of adjustable low-pass and band-pass circular filters are provided, for specified selectivity and peak frequency.

2 Gaussian Prototype Filters

Zero-phase filters (both FIR and IIR), in particular Gaussian filters are often used in image processing because they have the useful feature to yield filtered images free of any phase distortions. Furthermore, the 2D Gaussian is separable, therefore it can be implemented as a cascade of 1D filters. We begin our design with the 1D Gaussian prototype filter:

$$G(\omega)=\exp\left(-\sigma^2\omega^2/2\right) \quad (1)$$

This is the Fourier transform of Gaussian function in continuous spatial variable *x*:

$$g(x)=\left(1/\sqrt{2\pi}\sigma\right)\cdot\exp\left(-x^2/2\sigma^2\right) \quad (2)$$

For simplicity, instead of (1), we use the expression $G_P(\omega)=\exp(-p\,\omega^2)$, with $p=\sigma^2/2$, where p has the role of a selectivity parameter; the larger the value of *p*, the narrower is the Gaussian. A 1D band-pass (BP) Gaussian filter may be put into the form:

$$G_{BP}(\omega)=\exp\left(-p(\omega-\omega_0)^2\right)+\exp\left(-p(\omega+\omega_0)^2\right) \quad (3)$$

where ω_0 is the BP filter central or peak frequency. So $G_{BP}(\omega)$ is the sum of two elementary Gaussians $G(\omega)$ shifted around $-\omega_0$ and ω_0.

The design procedure presented as follows is based on a polynomial approximation of the 1D Gaussian prototype function $\exp(-p\,\omega^2)$.

A very efficient approximation (with best tradeoff between accuracy and approximation order) is given by the Chebyshev series method, which yields an uniform approximation of a given function over a specified range, unlike Taylor expansion. The single drawback is that the approximation coefficients are only derived numerically, with symbolic calculation software like MAPLE.

Thus, we intend to find a series expansion of the function $G_P(\omega)$, an approximation with an imposed precision on frequency interval $[-\pi,\pi]$. Generally, a given filter function $G_P(\omega)$ can be approximated to a specified accuracy on a given frequency range by a polynomial function $G_a(\omega)$ of order *N*:

$$G_P(\omega)\cong G_a(\omega)=\sum_{j=0}^{N}a_j\cdot\omega^j \quad (4)$$

The order *N* of polynomial $G_a(\omega)$ depends on filter selectivity, imposed precision of approximation and frequency interval. Generally the polynomial $G_a(\omega)$ will be factored as [14]:

$$G_a(\omega)=\alpha\cdot\prod_{i=1}^{N_1}(\omega^2-a_i)\cdot\prod_{j=1}^{N_2}(\omega^4-b_j\cdot\omega^2+c_j) \quad (5)$$

where $2N_1+4N_2=N$ is the order of polynomial approximation and α is a constant.

3 Gaussian Prototype Approximation and Frequency Mapping for Designing Circular Filters

In this section, 2D circular filters will be derived by applying a specific frequency transformation to the factored polynomial approximstion of the prototype frequency response. This procedure will be carried for two types of filters, namely low-pass (LP) and band-pass (BP).

3.1 Trigonometric prototype approximation through Chebyshev series

In order to find a trigonometric approximation as a polynomial in $\cos\omega$, first we make the following change of variable, also used in [18]:

$$\omega=\arccos\left(x/\pi\right)\leftrightarrow x=\pi\cos\omega \quad (6)$$

For Gaussian function $G_1(\omega)=\exp(-\omega^2)$, we will first find the Chebyshev series approximation for function $\exp(-(\arccos(\omega/\pi))^2)$, normally calculated on the frequency range $[-\pi,\pi]$.

The Chebyshev series is very useful and convenient, as it gives an approximation of a function which is uniform, basically with equal error along the entire specified interval, while the Taylor formula gives a polynomial approximation around a specified point and the approximation diverges rapidly towards the limits of given range. We use function "chebyshev" available in MAPLE software. The approximation is accurate on specified range $[-\pi,\pi]$, but it diverges rapidly outside it. Since we further use the function $G_a(\omega)$ for a 2D circular filter, obtained by rotating the 1D prototype around its axis, the approximation must hold on a larger range, namely $[-\pi\sqrt{2},\pi\sqrt{2}]$, otherwise circular filter characteristic will diverge towards the corners of the frequency plane, thus the shape will have large distortions.

Consequently, the variable change (6) will become:

$$\omega=\arccos\left(x/\pi\sqrt{2}\right)\leftrightarrow x=\pi\sqrt{2}\cdot\cos\omega \quad (7)$$

and we obtain, using a specified error of 0.01:

$$\exp\left(-\left(\arccos(x/\pi\sqrt{2})\right)^2\right)\cong 0.0848722+0.059327\cdot x +0.01717295\cdot x^2+0.0027913\cdot x^3+0.00022045\cdot x^4 \quad (8)$$

Substituting back *x* by $x=\pi\sqrt{2}\cdot\cos\omega$, we get the approximation as a polynomial in variable $\cos\omega$:

$$G_1(\omega)=\exp(-\omega^2)\cong 0.28209+.043937\cdot\cos\omega+0.20755\cdot\cos 2\omega+0.059444\cdot\cos 3\omega+0.010328\cdot\cos 4\omega \quad (9)$$

or in a factored form like:

$$\exp(-\omega^2)\cong 0.08263\cdot(\cos^2\omega+1.7948\cdot\cos\omega+0.8065)\cdot(\cos^2\omega+1.0829\cdot\cos\omega+1.2736) \quad (10)$$

Of course, for more selective Gaussian filters, which correspond to larger values of parameter p, more terms of the Chebyshev series need to be kept, to obtain an approximation with the same precision. For instance, following the same technique, we get for the function $G_2(\omega)=\exp(-4\omega^2)$:

$$\begin{aligned} G_2(\omega)=\exp(-4\omega^2) \cong\ & 0.141034+0.264921\cdot\cos\omega \\ & +0.21967\cdot\cos 2\omega+0.16065\cos 3\omega+0.103749\cdot\cos 4\omega \\ & +0.059048\cdot\cos 5\omega+0.029706\cdot\cos 6\omega \\ & +0.013113\cdot\cos 7\omega+0.00514\cdot\cos 8\omega \end{aligned} \quad (11)$$

or in factored form as previously:

$$\begin{aligned} G_2(\omega) \cong\ & 0.657931\cdot(\cos\omega+0.981717) \\ & \cdot(\cos\omega+0.856848)\cdot(\cos\omega+0.62376) \\ & \cdot(\cos\omega+0.31344)\cdot(\cos\omega-0.03907) \\ & \cdot(\cos\omega-0.283997) \\ & \cdot(\cos^2\omega-1.177115\cdot\cos\omega+0.457769) \end{aligned} \quad (12)$$

As a remark, the Gaussian $G_2(\omega)=\exp(-4\omega^2)$ can be regarded as a compressed version on frequency axis of the Gaussian $G_1(\omega)=\exp(-\omega^2)$ by factor 2 ($\omega\to 2\omega$) and the order of approximation is 8, (double); we expect that for $G_3(\omega)=\exp(-9\omega^2)$, the approximation order will be 12 (triple) and so on.

3.2 Parametric polynomial approximation using Chebyshev series

A somewhat different approach would be to design a parametric or adjustable filter, for which value p would appear explicitly in the filter transfer function and thus the design for new specifications reduces to a simple value substitution.

The idea is to make the filter function scalable on the frequency axis (within certain limits), by making $\omega\to p\cdot\omega$, where p can take arbitrary values; the scaling is a dilation for $p<1$, compression for $p>1$.

The trigonometric approximation (9) of Gaussian $G_1(\omega)=\exp(-\omega^2)$ cannot be practically scaled, as it would contain cosine terms of the form $\cos(pN\omega)$, generally with non-integer p, difficult to deal with. Using the efficient Chebyshev series as before, we obtain directly, without using the previous change of variable, the following polynomial approximation for $G_1(\omega)=\exp(-\omega^2)$, calculated on range $[-\pi,\pi]$:

$$\begin{aligned} & G_1(\omega)\cong\alpha\cdot(\omega^2-5.7968)(\omega^2-6.5916)(\omega^2-8.7431) \\ & (\omega^2-9.7236)(\omega^4-5.51094\cdot\omega^2+13.36003)=H_{G1}(\omega) \end{aligned} \quad (13)$$

where $\alpha=0.229375\cdot 10^{-4}$.

Compared to the trigonometric series (9) of order 4, we notice that the order is much higher, namely 12. Moreover, the approximation (plotted in red in Fig. 1 (a)) diverges very rapidly outside the interval.

For $G_2(\omega)=\exp(-4\omega^2)$ we get similarly, where the constant is $\beta=0.85705\cdot 10^{-6}$:

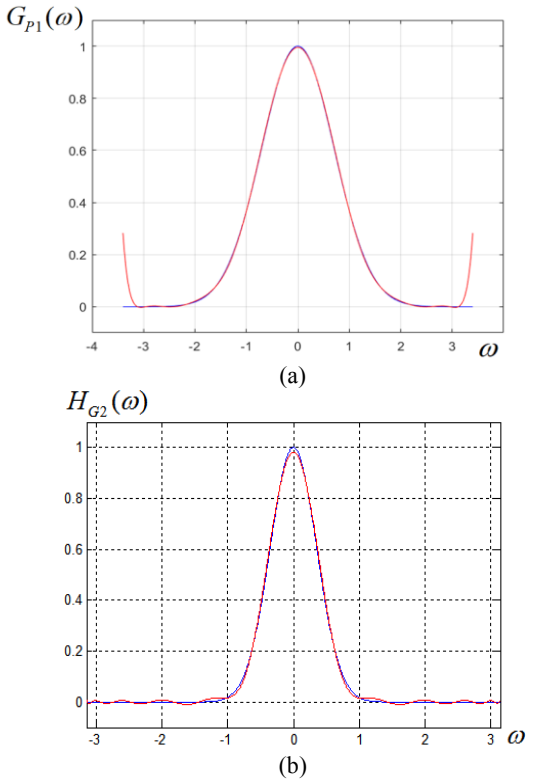

Fig.1: (a) Polynomial approximations for Gaussian $G_1(\omega)=\exp(-\omega^2)$; (b) similar for $G_2(\omega)=\exp(-4\omega^2)$

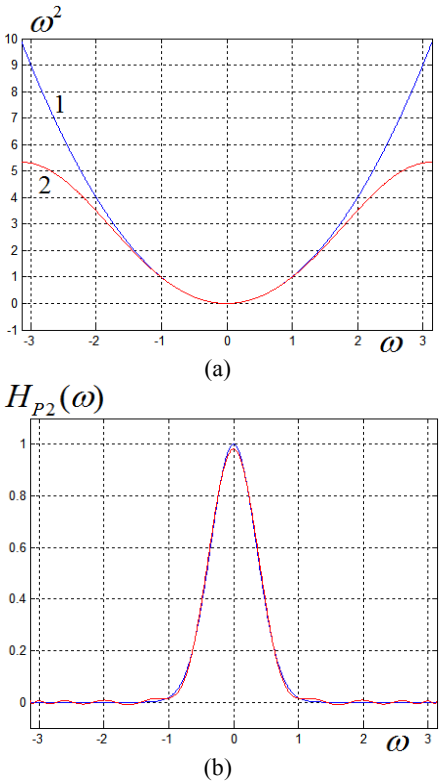

Fig.2: (a) Function ω^2 and its approximation using Taylor series; (b) prototype $G_2(\omega)$ and its approximation $H_{P2}(\omega)$

$$G_2(\omega) \cong \beta \cdot \left(\omega^2 - 2.0516\right)\left(\omega^2 - 3.28931\right)\left(\omega^2 - 4.68917\right)$$
$$\left(\omega^2 - 6.1195\right)\left(\omega^2 - 7.4554\right)\cdot\left(\omega^2 - 8.5736\right)\left(\omega^2 - 9.386\right) \quad (14)$$
$$\left(\omega^2 - 9.8045\right)\left(\omega^4 - 1.89305\cdot\omega^2 + 1.00547\right) = H_{G2}(\omega)$$

which is plotted in Fig.1(b). The approximations are polynomials in even powers of frequency ω, and they can be scaled with factor *p*, making $\omega \to p\cdot\omega$.

Next, we look for a simple approximation of ω^2 as a cosine series. While the Chebyshev series expansion is generally more convenient, in this case a precise approximation of ω^2 is not needed on entire range $[-\pi,\pi]$, but rather around zero. The variable change $\omega = \arccos x \leftrightarrow x = \cos\omega$ is first used. In this way, we find the Taylor series of $(\arccos x)^2$ around the point $x = 1$, truncated to the second-order term as:

$$(\arccos x)^2 \cong -2(x-1) + (1/3)\cdot(x-1)^2 = 7/3 - (8/3)\cdot x + (1/3)\cdot x^2 \quad (15)$$

Substituting back in (15) the variable $x = \cos\omega$ and using trigonometric identities, the following simple approximation is found [18]:

$$\omega^2 \cong 2.5 - 2.66667\cdot\cos\omega + 0.166667\cdot\cos 2\omega \quad (16)$$

As can be noticed, this approximation (curve 2 from Fig.2 (a)) is precise around zero, diverging towards the limits of the range $[-\pi,\pi]$ with a large error as compared to the original function ω^2 (curve 1). However, by replacing back the expression (16) into each scaled factor of $G_1(\omega)$ from (14), the marginal errors cancel away, resulting in an accurate overall approximation, shown in Fig.2 (b) where $G_2(\omega)$ (in blue) and approximation $H_{P2}(\omega)$ (red) are practically superposed. Therefore, we expect the resulting 2D circular filter to be also very accurate in shape. Thus a uniform approximation on the entire range $[-\pi,\pi]$ is not necessary. The advantage is the low order of approximation, which leads to a more efficient, low-order 2D filter, convenient for implementation.

3.3 Frequency mapping for circular filter

This analytical design approach uses a 1D to 2D frequency mapping which, applied to the prototype, leads directly to the frequency response or transfer function of the 2D filter with desired circular shape. Starting from a 1D prototype with transfer function $H_p(\omega)$, a circularly-symmetric 2D filter $H(\omega_1,\omega_2)$ simply results by applying the 1D to 2D frequency transformation $\omega \to \sqrt{\omega_1^2 + \omega_2^2}$:

$$H(\omega_1,\omega_2) = H_p\left(\sqrt{\omega_1^2 + \omega_2^2}\right) \quad (17)$$

which can be regarded as a *rotation* of the prototype around its central axis, generating 2D characteristic.

A commonly used approximation of the 2D function $\cos\sqrt{\omega_1^2 + \omega_2^2}$ corresponds to the 3×3 matrix:

$$C = \begin{bmatrix} 0.125 & 0.25 & 0.125 \\ 0.25 & -0.5 & 0.25 \\ 0.125 & 0.25 & 0.125 \end{bmatrix} \quad (18)$$

such that the following approximation is valid:

$$\cos\sqrt{\omega_1^2 + \omega_2^2} \cong C(\omega_1,\omega_2) = -0.5 + 0.5(\cos\omega_1 + \cos\omega_2) + 0.5\cos\omega_1\cos\omega_2 \quad (19)$$

This is in fact a simple particular case of McClellan transform. The function $C(\omega_1,\omega_2)$ and constant level contours are displayed in Fig.3, showing a precise circular shape throughout a large domain, while near margins the contour circularity is visibly distorted, its shape looking more like a rounded square. The circular cosine function decreases smoothly and uniformly to the minimum value (-1) near frequency plane margins, with no visible ripple. Moreover, the deviation from circularity is rather unimportant for the filters under discussion, as will be shown in the following design examples.

Let us consider a FIR filter $H_P(\omega)$ with frequency response given by the following expression [14]:

$$H_P(\omega) = b_0 + 2\sum_{k=1}^{R} b_k \cos k\omega \quad (20)$$

Using trigonometric identities for $\cos k\omega$, $k = 1\ldots R$, we get a polynomial expression in powers of $\cos\omega$:

$$H_P(\omega) = c_0 + \sum_{k=1}^{R} c_k (\cos\omega)^k \quad (21)$$

Considering this polynomial form of the prototype and applying the frequency transformation specified previously, we obtain the frequency response of the corresponding 2D circular filter [14]:

$$H(\omega_1,\omega_2) = H_P\left(\sqrt{\omega_1^2 + \omega_2^2}\right) = c_0 + \sum_{k=1}^{R} c_k \cdot C^k(\omega_1,\omega_2) \quad (22)$$

where notation $C(\omega_1,\omega_2) = \cos\sqrt{\omega_1^2 + \omega_2^2}$ defined in (19) was used. Thus, starting from a convenient 1D prototype filter with desired frequency response, the design of the 2D circular filter simply consists in replacing $\cos\omega$ in the prototype function $H_P(\omega)$

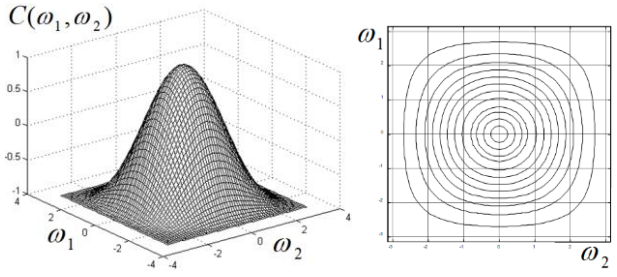

Fig.3: Characteristic and contours of circular cosine $C(\omega_1,\omega_2)$

with the *circular cosine* $C(\omega_1,\omega_2)=\cos\sqrt{\omega_1^2+\omega_2^2}$. Supposing that the prototype $H_P(\omega)$ is factored into first and second-order polynomial factors in $\cos\omega$, and making the above substitution in each factor of $H_P(\omega)$, we obtain the circular frequency response $H(\omega_1,\omega_2)$ in factored form as [14]:

$$H(\omega_1,\omega_2)=k\cdot\prod_{i=1}^{n}(C+b_i)\cdot\prod_{j=1}^{m}(C^2+b_{1j}\cdot C+b_{2j}) \quad (23)$$

where C is a shorthand notation for $C(\omega_1,\omega_2)$.

Since the given prototype filter can be expressed as a product of elementary functions, the circular filter will also have a factored transfer function, a major advantage in implementation. The large-size kernel **H** corresponding to the FIR filter $H(\omega_1,\omega_2)$ results directly decomposed into elementary, small-size (3×3 or 5×5) matrices, as discrete convolution [14]:

$$\mathbf{H}=k\cdot(\mathbf{C}_1*\ldots*\mathbf{C}_i*\ldots*\mathbf{C}_n)*(\mathbf{D}_1*\ldots*\mathbf{D}_j*\ldots*\mathbf{D}_m) \quad (24)$$

The above relation is a matrix form of (23). Using the 3×3 matrix **C** from (18) and according to (23), each 3×3 matrix $\mathbf{C}_i$ from (24) is obtained from **C** by adding value b_i occurring in each factor in (23) to the central element of matrix **C**. Then, each 5×5 template $\mathbf{D}_j$ is given by the expression [14]:

$$\mathbf{D}_j=\mathbf{C}*\mathbf{C}+b_{1j}\cdot\mathbf{C}_1+b_{2j}\cdot\mathbf{C}_0 \quad (25)$$

$\mathbf{C}_0$ is a 5×5 zero matrix, with central element one; $\mathbf{C}_1(5\times5)$ results by bordering **C** (3×3) with zeros, and the symbol * represents matrix convolution.

4 Gaussian Circular Filter Design

In this section, 2D circular FIR filters of LP and BP type will be designed in two versions, one being parametric or adjustable.

4.1 Separable low-pass circular filters

For a simple low-pass filter of this kind, we use the 2D Gaussian property to be separable into two 1D Gaussian functions along the frequency axes. Indeed from the Gaussian prototype $G_1(\omega)=\exp(-p\cdot\omega^2)$ we derive the separable circular filter:

$$\begin{aligned}G_C(\omega_1,\omega_2)&=\exp\left(-p\left(\omega_1^2+\omega_2^2\right)\right)\\&=\exp\left(-p\,\omega_1^2\right)\cdot\exp\left(-p\,\omega_2^2\right)\end{aligned} \quad (26)$$

Thus, a 2D Gaussian circular filtering can be simply reduced to applying a Gaussian 1D filtering on each frequency axis. Using prototypes $G_1(\omega)=\exp(-\omega^2)$ and $G_2(\omega)=\exp(-4\omega^2)$ given by (9) and (11) and applying each on both axes, two Gaussian circular filters are derived, whose frequency responses and contour plots are shown in Fig.4, along with their prototypes. There can be noticed the very accurate Gaussian shape and circularity of the characteristics in the frequency plane, and also the absence of any ripple in the stop band, as show the level contours.

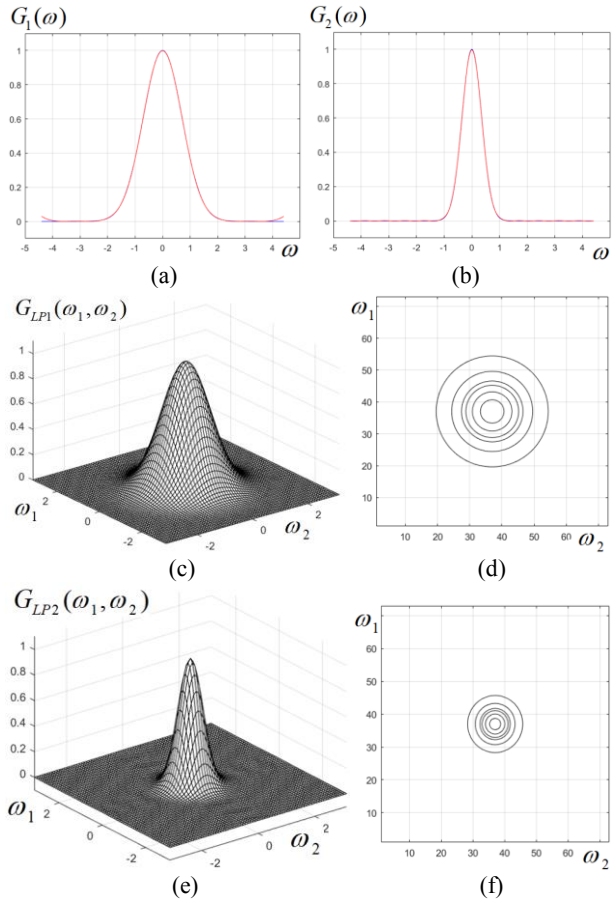

Fig.4: (a), (b) Prototype approximations for *p*=1 and *p*=4; (c)-(f) characteristics and contour plots of circular filters

4.2 Adjustable low-pass circular filters

The presented design procedure is quite simple and efficient, leading in a straightforward manner to the factored frequency response of the low-pass filter. However, changing the filter selectivity through the value *p*, we have to resume each time all the design steps, which may become tedious.

Of course these parametric LP Gaussian filters are also separable and are designed following the steps described in detail in sub-section 3.2. In Fig.5, the characteristics and level contours are plotted for the specified values of scaling parameter *p*. For *p*=1 we have the trivial case, where filter characteristics result practically identical with the one designed previously. As we notice, for values of *p* between 0.5 and 2 the filter response has a correct shape and good circularity, with some ondulations in the stop band, visible at *p*=0.5 and *p*=2. Therefore, in this

version, the filter results adjustable with value *p*. Similarly, if we need a Gaussian circular filter to be adjusted in the range [2,8], we should use the prototype $G_2(\omega)=\exp(-4\omega^2)$, and so on. Of course, the larger the value *p*, the higher will be the filter order.

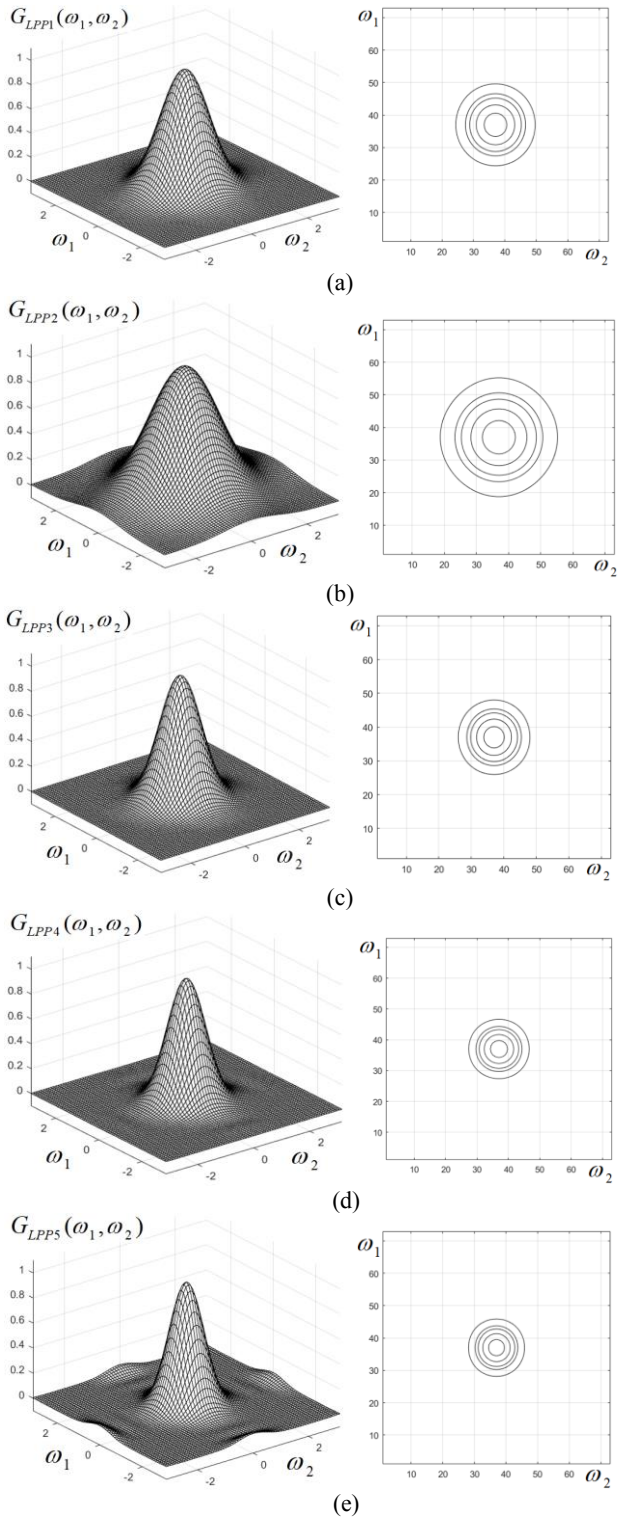

Fig.5: Characteristics and level contours of parametric Gaussian circularfilters for scale parameter values: (a) p=1; (b) p=0.5; (c) p=1.3; (d) p=1.7; (e) p=2

4.3 Adjustable band-pass circular filters

Using this analytical design method applied to the Gaussian prototype, we can also obtain band-pass (BP) circular filters, with specified selectivity value *p* and peak frequency ω_0.

In order to obtain the 1D prototype for a BP filter, two Gaussians shifted around the frequencies $\pm\omega_0$ are summed together, resulting in the BP prototype:

$$G_{BP}(\omega)=\exp\left(-p\cdot(\omega-\omega_0)^2\right)+\exp\left(-p\cdot(\omega+\omega_0)^2\right) \quad (27)$$

Let us consider the procedure detailed in sub-section 3.1, applied for a specified value of scale parameter *p*. The relation (9) for *p*=1 is written simpler as:

$$G_1(\omega)=\exp(-\omega^2)\cong a_0+a_1\cos\omega+a_2\cos 2\omega+a_3\cos 3\omega+a_4\cos 4\omega \quad (28)$$

Making $\omega\to\omega\pm\omega_0$, we obtain the BP prototype:

$$G_{BP1}(\omega)=\exp(-(\omega-\omega_0)^2)+\exp(-(\omega+\omega_0)^2) \quad (29)$$

which, taking into account (28), can be written:

$$\begin{aligned}G_{BP1}(\omega)\cong\ & 2a_0+a_1\cos(\omega-\omega_0)+a_1\cos(\omega+\omega_0)\\ &+a_2\cos 2(\omega-\omega_0)+a_2\cos 2(\omega+\omega_0)\\ &+a_3\cos 3(\omega-\omega_0)+a_3\cos 3(\omega+\omega_0)\\ &+a_4\cos 4(\omega-\omega_0)+a_4\cos 4(\omega+\omega_0)\end{aligned} \quad (30)$$

It is easy to re-arrange (30) as follows:

$$\begin{aligned}G_{BP1}(\omega)\cong 2\cdot(a_0+&a_1\cos\omega_0\cdot\cos\omega+a_2\cos 2\omega_0\cdot\cos 2\omega\\ &+a_3\cos 3\omega_0\cdot\cos 3\omega+a_4\cos 4\omega_0\cdot\cos 4\omega)\end{aligned} \quad (31)$$

In the general case, the BP prototype can be written:

$$G_{BP}(\omega)=2\cdot\sum_{n=0}^{N}a_n\cos\omega_0\cdot\cos(n\cdot\omega) \quad (32)$$

Since the BP filters are no longer separable, we use the procedure presented in sub-section 3.3.

The filter with *p*=1 is too wide and an efficient BP filter results only for $\omega_0=0.5\pi$ or close to it. The expression (32) is a function of two variables, ω_0 and ω, and generally cannot be factored. Instead, to get a more efficient filter, a nested implementation may be approached.

Mathematically, this corresponds to a Horner polynomial form, which is the following:

$$\begin{aligned}P(x)&=a_0+a_1x+a_2x^2+a_3x^3\ldots+a_nx^n\\ &=a_0+x\left(a_1+x\left(a_2+x\left(a_3+\ldots+x\left(a_{n-1}+a_nx\right)\ldots\right)\right)\right)\end{aligned} \quad (33)$$

Referring to the more selective BP filter with *p*=4, given by the expression:

$$\begin{aligned}G_{BP2}(\omega)&=\exp\left(-4(\omega-\omega_0)^2\right)+\exp\left(-4(\omega+\omega_0)^2\right)\\ &\cong 2\cdot(a_0+a_1\cos\omega_0\cdot\cos\omega+a_2\cos 2\omega_0\cdot\cos 2\omega\\ &\quad+a_3\cos 3\omega_0\cdot\cos 3\omega+\ldots+a_8\cos 8\omega_0\cdot\cos 8\omega)\end{aligned} \quad (34)$$

and using trigonometric identities for $\cos n\omega$, after re-arranging terms, we obtain the following Horner

form of the BP filter function, for order 8:

$$G_{BP}(\omega) = h_0 + (h_1 + (h_2 + \ldots (h_7 + h_8 \cos\omega)\cdot\cos\omega)\ldots)\cdot\cos\omega \quad (35)$$

where the Horner coefficients depend on $\cos\omega_0$ and have the following polinomial expressions in the variable s, where $s = \cos\omega_0$:

$$\begin{aligned}
h_0 &= 0.9985934 - 0.937027\cdot s^2 + 6.156547\cdot s^4 \\
&\quad - 4.532877\cdot s^6 + 1.315863\cdot s^8 \\
h_0 &= 7.659075\cdot s - 25.946093\cdot s^3 + 30.00929\cdot s^5 \\
&\quad - 11.749434\cdot s^7 \\
h_2 &= -3.937027 + 44.813339\cdot s^2 - 117.24553\cdot s^4 \\
&\quad + 118.4359367\cdot s^6 - 42.1076054\cdot s^8 \\
h_3 &= -25.94609\cdot s + 134.625769\cdot s^3 \\
&\quad - 202.283215\cdot s^5 + 93.995476\cdot s^7 \\
h_4 &= 6.156547 - 117.24553\cdot s^2 + 413.335372\cdot s^4 \\
&\quad - 512.331323\cdot s^6 + 210.538027\cdot s^8 \\
h_5 &= 30.00929 - 202.283215\cdot s^2 + 359.217071\cdot s^4 \\
&\quad - 187.99095\cdot s^6 \\
h_6 &= -4.532877 + 118.435937\cdot s^2 - 512.331323\cdot s^4 \\
&\quad + 734.55853\cdot s^6 - 336.860843\cdot s^8 \\
h_7 &= -11.749434 + 93.995476\cdot s^2 - 187.99095\cdot s^4 \\
&\quad + 107.4234\cdot s^6 \\
h_8 &= 1.315863 - 42.1076054\cdot s^2 + 210.53803\cdot s^4 \\
&\quad - 336.860843\cdot s^6 + 168.43042\cdot s^8
\end{aligned} \quad (36)$$

As a numerical example, for the BP filter with p=4 and $\omega_0 = 0.5\pi$, we have $s = \cos\omega_0 = 0$ and in this case the Horner decomposition is the following:

$$\begin{aligned}
G_{BP}(\omega) &= \exp\left(-4(\omega-\pi/2)^2\right) + \exp\left(-4(\omega+\pi/2)^2\right) \\
&= 0.998593 + (-3.93703 + (6.1565473 \\
&\quad + (-4.5329 + 1.31586\cdot\cos^2\omega)\cdot\cos^2\omega)\cdot\cos^2\omega)\cdot\cos^2\omega
\end{aligned} \quad (37)$$

For the BP filter with p=4 and $\omega_0 = 0.3\pi$, we have $s = \cos\omega_0 \cong 0.5878$ and the Horner decomposition is given now by the general formula (35), with the coefficient values: $h_0 = 0.205071$, $h_1 = 1.05356$, $h_2 = 1.8349$, $h_3 = 0.1745$, $h_4 = -3.14178$, $h_5 = -2.7936$, $h_6 = 0.724816$, $h_7 = 1.59634$, $h_8 = 0.406624$.

Gaussian-shaped band-pass filters are not separable, unlike their low-pass counterparts. However, in this case the 2D filter results directly through a simple substitution. In the factored prototype frequency response or in its Horner polynomial form, we simply replace $\cos\omega$ by the circular cosine function $C(\omega_1,\omega_2)$ discussed previously, given by (19).

Referring again to the general Horner form given in (35), this corresponds to a filter kernel resulting in an iterative manner as:

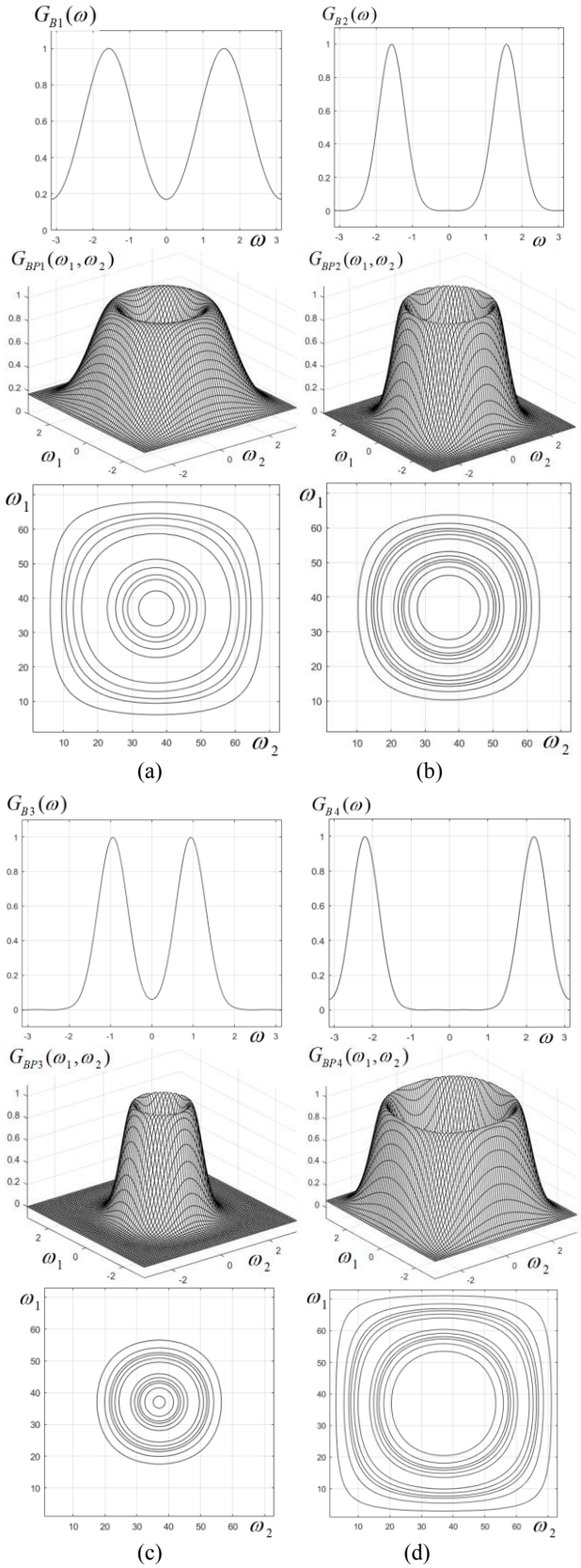

Fig.6: 1D prototypes, characteristics and constant level contours for Gaussian circular band-pass filters with parameters: (a) $p=1,\ \omega_0 = 0.5\pi$; (b) $p=4,\ \omega_0 = 0.5\pi$; (c) $p=4,\ \omega_0 = 0.3\pi$; (d) $p=4,\ \omega_0 = 0.7\pi$

$$\mathbf{G}_{BP} = h_0 + (h_1 + (h_2 + \ldots (h_7 + h_8 \cdot \mathbf{C}) * \mathbf{C}) * \mathbf{C} \ldots) * \mathbf{C} \quad (38)$$

In this expression, the symbol $*$ means convolution of matrices. For instance, in the case of the circular BP filter discussed before, with p=4 and $\omega_0 = 0.3\pi$, the kernel results of size 17×17, through successive convolution of elementary matrices of size 3×3. As shows (38), in the first step, the matrix $\mathbf{C}$ given by (18) is multiplied by the coefficient h_8, then h_7 is added to its central element; the resulted 3×3 matrix is convolved with $\mathbf{C}$, then h_5 is added to its central element, obtaining a matrix of size 5×5, and so on, until the overall filter kernel is obtained. This nested implementation, based on Horner form of the prototype frequency response, is the most efficient, as it requires the minimum number of operations.

In Fig.6, the 1D prototypes, filter characteristics and level contours are shown for several BP circular filters with specified parameters (selectivity given by p and peak frequency of value ω_0).

5 Comparative Discussion

This work presented an analytical design method in the frequency domain for parametric circular filters. The proposed design procedure uses some efficient polynomial and trigonometric approximations, like Chebyshev series, which are easily calculated for a specified precision using a symbolic computation software, for instance MAPLE. An optimal trade-off is necessary between accuracy and complexity. For a high precision imposed, the filter would result of a large order and its kernel would be of a large size, therefore difficult to implement. Anyway, as shown, the filter kernel results directly decomposed into small-size matrices, which implies that the desired 2D filter can be implemented as a cascade structure of elementary filters and achieved in several stages. The novelty of this approach as compared with other works on the topic consists in designing Gaussian circular LP and BP filters, adjustable in selectivity and peak frequency, based on frequency mappings applied to Gaussian prototypes, which differs from previous works. The circular FIR filters in [14] are based on the Fourier series. The Gaussian circular filter bank proposed in [15] is of IIR type, as well as the filter bank developed in [16], based on a digital prototype, with a complex frequency response of the 2D filter. A new aspect is also the nested realization, which allows for an efficient implementation of the designed circular filter. The Gaussian prototype has several advantages. It is a smooth function, easy to develop in a polynomial or trigonometric series and leads to separable circular filters. Moreover, it it one of the most commonly used as it yields zero-phase 2D filters, widely used in image processing as they do not introduce any phase distortions in the filtered image. In many works on this topic, Gaussian filters are designed and implemented as IIR filters, due to their advantages, mainly high processing speed and reduced computational complexity [9], [10].

Compared to other relatively recent methods used in circular filter design, employing techniques such as global optimization on intervals combined with McClellan transform [2], nature-inspired, heuristic approaches such as Levy flight algorithm [3], semi-definite programming [5], 2-D Laguerre distributed approximating functional [7] or sampling-kernel-based interpolation [8], the technique proposed here is substantially simpler, but yielding very efficient 2D parametric circular filters with tuning capability.

The main reason why a FIR version was developed here is that FIR filters are unconditionally stable. It is more difficult to design stable 2D IIR filters in closed form, using analytical methods, due to stability restrictions. Even if one starts from a stable prototype, the applied frequency mappings may not preserve stability, therefore for the 2D IIR filters the stability is difficult to guarantee [18].

The purpose of this paper was mainly to present this analytic method and to give some design examples for LP and BP circular filters. Their image filtering capabilities are quite well known, that is why image filtering examples were not included in this work.

6 Conclusion

A simple and efficient analytical design method for 2D Gaussian circular FIR filters was proposed, that starts from a specified prototype and yields a 2D filter with a frequency response in a factored, closed form. This design procedure is based on Chebyshev series approximations and on a specific frequency mapping expressed conveniently in matrix form and does not involve any global numerical optimization. The main advantage of this technique is that it leads to parametric, adjustable filters, since the 2D filter frequency response already contains explicitly the design specifications. For instance, to change filter selectivity we simply substitute the new parameter value, thus avoiding the need to resume the design procedure every time for different specifications.

The low-pass filters are adjustable in selectivity, while the band-pass filters are tunable to a desired peak frequency. The filters have accurate shape, good circularity and relatively low order. A nested filter realization is presented, very efficient in implementation due to minimum number of operations required. Further work on this topic will focus on applying this method also to other FIR filters with various shapes.

References:

[1] W. Lu, A. Antoniou, *Two-Dimensional Digital Filters (Electrical and Computer Engineering, new edition)*, CRC Press, 2020

[2] Y. Wang, J. Yue, Y. Su, H.Liu, Design of Two-Dimensional Zero-Phase FIR Digital Filter by McClellan Transformation and Interval Global Optimization, *IEEE Trans. Circ. and Systems II: Express Briefs*, 60 (3), 2013, pp. 167-171

[3] M. Hussain, W.K. Jenkins, C. Radhakrishnan, Use of the Lévy Flight Firefly Algorithm in 2D McClellan Unconstrained Transform Adaptive Filters, *IEEE 63rd Intl. Midwest Symposium on Circuits and Systems*, 9-12 August 2020, Springfield, MA, USA, pp. 856-859

[4] M. T. Hanna, Design of Circularly Symmetric Two-Dimensional Linearphase Low-Pass FIR Filters Using Closed-Form Expressions, *IEEE Trans. on Circuits and Systems II*, Vol. 43 (7), July 1996, pp. 537-540

[5] T. Q. Hung, H. D. Tuan, T. Q. Nguyen, Design of Diamond and Circular Filters by Semi-definite Programming", *Proc. ISCAS 2007*, pp. 2966-2969

[6] K.R.Sreelekha, T.S.Bindiya, A New Multiplier-Free Transformation for the Design of Hard-ware Efficient Circularly Symmetric Wideband 2D Filters, *IEEE TENCON 2019*, 17-20 Oct. 2019, Kochi, India, pp. 2376-2381

[7] Soo-Chang Pei, Shih-Gu Huang, 2-D Laguerre Distributed Approximating Functional: A Circular Low-Pass/Band-Pass Filter, *IEEE Trans. Circ. Syst. II: Express Briefs*, 66 (5), 2019, pp. 818 – 822

[8] K.J. Kim, J.H. Kim, S.W. Nam, Design of Computationally Efficient 2D FIR Filters Using Sampling-Kernel-Based Interpolation and Frequency Transformation, *Electronics Letters*, 51 (17), 2015, pp. 1326-1328

[9] J.-M. Geusebroek, A.W.M. Smeulders, J. van de Weijer, Fast Anisotropic Gauss Filtering, *IEEE Trans. on Image Processing*, Vol. 12 (8), August 2003, pp.938-943

[10] S.Y. Lam, B.E. Shi, Recursive Anisotropic 2-D Gaussian Filtering Based on a Triple-Axis Decomposition, *IEEE Transactions on Image Processing*, 16 (7), 2007, pp. 1925-1930

[11] Z. Jainguo, T. Tieniu, Ma Li, Invariant Texture Segmentation via Circular Gabor Filters", the *16-th International. Conference on Pattern Recognition*, 11-15 Aug.2002, Quebec, Canada, Vol.2, pp. 901-904

[12] B.Tirumala Krishna, Novel Digital Integrators and Differentiators Using Fractional Delay - A Biomedical Application, *International Journal of Circuits, Systems and Signal Processing*, Volume 13, 2019, pp. 379-384

[13] P.Kamala Kumari, Dr.J.B.Seventline, Improved Spectral Characteristics of Bandpass FIR Filter using a Novel Adjustable Window Function, *International Journal of Circuits, Systems and Signal Processing*, Vol. 13, 2019, pp. 662-666

[14] R. Matei, L. Goraş, A Class of Circularly-Symmetric CNN Spatial Linear Filters, *Facta Universitatis* (*Scientific Journal of University of Nis, Serbia*), *Electronics and Energetics*, Vol.19, No.2, 2006, pp.299-3163

[15] R. Matei, Parametric 2D Gaussian Circular Band-Pass Filters, *Proc. of IEEE International Symposium on Signals, Circuits and Systems, ISSCS 2013*, 11-12 July 2013, Iaşi, Romania, pp.1-4

[16] R. Matei, D. Matei, Circular IIR Filter Design and Applications in Biomedical Image Analysis, *Proc. of 10th IEEE International Conference on Electronics, Computers and Artificial Intelligence ECAI 2018*, 28-30 June 2018, Iaşi, Romania, pp.1-6

[17] R. Matei, Analytic Design of Directional and Square-Shaped 2D IIR Filters Based on Digital Prototypes, *Multidimensional Syst. and Signal Processing*, 30 (4), 2019, pp. 2021-2043

[18] R. Matei, Analytical Design Methods for Directional Gaussian 2D FIR Filters, *Multi-dimensional Systems and Signal Processing*, 29 (4), 2018, pp.185-211

Creative Commons Attribution License 4.0 (Attribution 4.0 International, CC BY 4.0)

This article is published under the terms of the Creative Commons Attribution License 4.0
https://creativecommons.org/licenses/by/4.0/deed.en_US